and modification of water masses. Applications to the wider problems are being explored.

See also

Estuarine Circulation. River Inputs. Tracers of Ocean Productivity. Water Types and Water Masses.

Further Reading

Alibo DS and Nozaki Y (1999) Rare earth elements in seawater: particle association, shale-normalization, and Ce oxidation. *Geochimica et Cosmochimica Acta* 63: 363–372.

Alibo DS and Nozaki Y and Jeandel C (1999) Indium and yttrium in North Atlantic and Mediterranean waters: comparison to the Pacific data. *Geochimica et Cosmochimica Acta* 63: 1991–1999.

Bertram C and Elderfield H (1993) The geochemical balance of the rare earth elements and neodymium isotopes in the oceans. *Geochimica et Cosmochimica Acta* 57: 1957–1986.

Byrne RH and Sholkovitz ER (1996) Marine chemistry and geochemistry of the lanthanides. In: Gschneider Jr KA and Eyring L (eds) *Handbook on the Physics and Chemistry of Rare Earths*, vol. 23, pp. 497–593. Amsterdam: Elsevier Science.

DeBaar HJW, Bacon MP and Brewer PG (1983) Rare-earth distributions with a positive Ce anomaly in the western North Atlantic Ocean. *Nature* 301: 324–327.

Elderfield H and Greaves MJ (1982) The rare earth elements in seawater. *Nature* 296: 214–219.

German CR, Holliday BP and Elderfield H (1991) Redox cycling of rare earth elements in suboxic zone of the Black Sea. *Geochimica et Cosmochimica Acta* 55: 3553–3558.

Goldberg ED, Koide M, Schmitt RA and Smith RH (1963) Rare-earth distributions in the marine environment. *Journal of Geophysical Research* 68: 4209–4217.

Greaves MJ, Statham PJ and Elderfield H (1994) Rare earth element mobilization from marine atmospheric dust into seawater. *Marine Chemistry* 46: 255–260.

Lipin BR and McKay GH (eds) (1989) Geochemistry and mineralogy of rare earth elements. *Reviews in Mineralogy* 21, Washington, DC: Mineralogical Society of America.

Nozaki Y (1997) A fresh look at elemental distribution in the North Pacific Ocean. *EOS Transactions* 78: 221.

Nozaki Y, Alibo DS, Amakawa H, Gamo T and Hasumoto H (1999) Dissolved rare earth elements and hydrography in the Sulu Sea. *Geochimica et Cosmochimica Acta* 63: 2171–2181.

Sholkovitz ER, Landing WM and Lewis BL (1994) Ocean particle chemistry: The fractionation of rare earth elements between suspended particles and seawater. *Geochimica et Cosmochimica Acta* 58: 1567–1579.

Sholkovitz ER and Schneider DL (1992) Cerium redox cycles and rare earth elements in the Sargasso Sea. *Geochimica et Cosmochimica Acta* 55: 2737–2743.

Taylor SR and McLennan SM (1985) *The Continental Crust: Its Composition and Evolution*. Oxford: Blackwell.

RED SEA CIRCULATION

D. Quadfasel, Niels Bohr Institute, Copenhagen, Denmark

doi:10.1006/rwos.2001.0377

Introduction

The Red Sea is a fiord type marginal sea in the north-west of the Indian Ocean, exposed to the arid climate of northern Africa and Arabia. Strong evaporation leads to a buoyancy-driven overturning circulation and to the production of a dense and highly saline water mass, the Red Sea Water. Near the surface the circulation is substantially modified through the forcing by the monsoon winds. Red Sea water spills at a rate of $0.37 \times 10^6\,m^3\,s^{-1}$ through the Strait of Bab El Mandeb into the Gulf of Aden and spreads at intermediate depths in the Indian Ocean, where it can be traced as far south as the southern tip of Africa. The circulation of the Red Sea appears not to be controlled by the hydraulics in the strait. This article summarizes the circulation internal to the Red Sea, the formation and transformation of the deep water masses and the exchange of water between the Red Sea and the Gulf of Aden.

The Red Sea was created as part of the spreading rift system between the African and the Arabian plates. It stretches between 12° and 20°N from tropical to subtropical latitudes (**Figure 1**), is about 2000 km long, on average 220 km wide and reaches depths of up to 2900 m, but its mean depth is only 560 m. The only connection to the oceans is in the south to the Gulf of Aden–Indian Ocean via the narrow Strait of Bab El Mandeb. The shallow Hanish sill of 163 m depth in the north of the strait limits the free communication to the upper part of the water column. Northern appendices to the Red Sea are the Gulf of Suez, a shallow shelf basin, and the 1800 m deep Gulf of Aqaba, a smaller version of the Red Sea itself, bounded by a 260 m deep sill

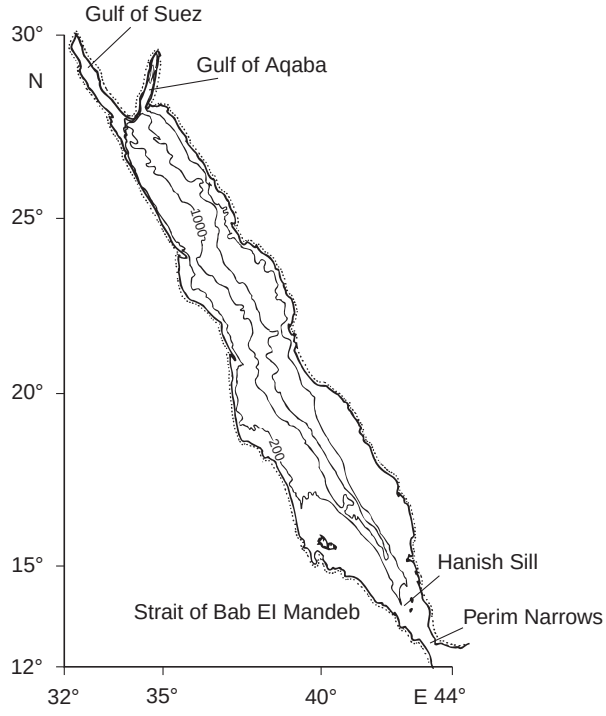

Figure 1 Bathymetry of the Red Sea with 200 m and 1000 m depth contours. Geographical names mentioned in the text are indicated.

in the Strait of Tiran. Both regions are important for the production of the deep water of the Red Sea.

The circulation of the Red Sea is driven by local atmospheric forces, through buoyancy and momentum fluxes. The net evaporative freshwater flux in the Red Sea is among the highest in the world, reaching $2\,\mathrm{m\,year^{-1}}$ with some seasonal variability associated with the monsoon wind system. During summer, values are highest in the north, but during winter in the south. Although the strong evaporation leads to sea surface salinities of up to 42 PSU (practical salinity units) in the Gulf of Suez, the buoyancy flux associated with the latent and sensible heat losses is an order of magnitude larger than that caused by the freshwater flux. In the north, where convection and water mass formation take place, the total buoyancy flux amounts to more than $20 \times 10^{-8}\,\mathrm{m^2\,s^{-3}}$. Here surface temperatures may drop below 20°C in winter.

The surface wind field over the Red Sea is guided by the high mountains and plateaux on either side of the basin, and its dominant component is in the along-axis direction. In the southern part winds reverse twice per year. During the south-west monsoon from June to September they blow towards south south-east, whereas during the north-east monsoon and the transition times between the monsoon periods (October to May) the airflow is directed towards north north-west. North of about 20°N the wind is blowing towards south south-east throughout the year, being strongest during summer and weakest during winter. Laterally the mean wind stress decreases from the central axis towards the boundaries on either side, due to lateral friction effects.

The geographical setting of the Red Sea with a length to width ratio of about ten has frequently led to the use of a two-dimensional channel approach to model the circulation. Also most of the observational data have been collected along the main axis of the Red Sea, limiting the interpretation of physical features to the two channel dimensions. The more recent three-dimensional surveys and modeling studies have, however, shown that at least in the upper layers significant cross-axis flows exist. Mesoscale gyres and eddies are an important part of the Red Sea circulation.

Hydrographic Structure

In terms of the classical hydrographic parameters the Red Sea can be viewed as a two-layer system consisting of a deep layer below sill depth, which is very homogeneous in temperature and salinity, and an upper layer, comprising the surface mixed layer and the strongly stratified thermocline. This upper layer is about 200–300 m deep. It is composed of warm and relatively fresh surface water that enters from the Indian Ocean and is then modified due to air–sea interaction. Evaporation increases the salinity, from 36 PSU in the Strait of Bab El Mandeb to above 40 PSU in the north, and cools the surface water, although locally some heating may also take place due to radiative heat gain. Convection and vertical mixing renews the subsurface water which then returns southward in the lower part of the thermocline.

The temperature and salinity distribution of the upper layer changes substantially between the two monsoon seasons, due to the varying atmospheric forcing (**Figure 2**). In winter the vertical temperature stratification is stable throughout the Red Sea. Highest surface temperatures are found around 18°N, in the zone of wind convergence and thus low wind speeds. Toward the north, surface temperatures decrease to less than 20°C in the Gulf of Suez. In the thermocline below the mixed layer, temperatures decrease to the deep water value. This pattern is consistent with the above described overturning circulation, typical for concentration basins, with an inflow at the surface and an outflow of colder and more saline, and thus denser water in the lower thermocline. It is this water that constitutes the

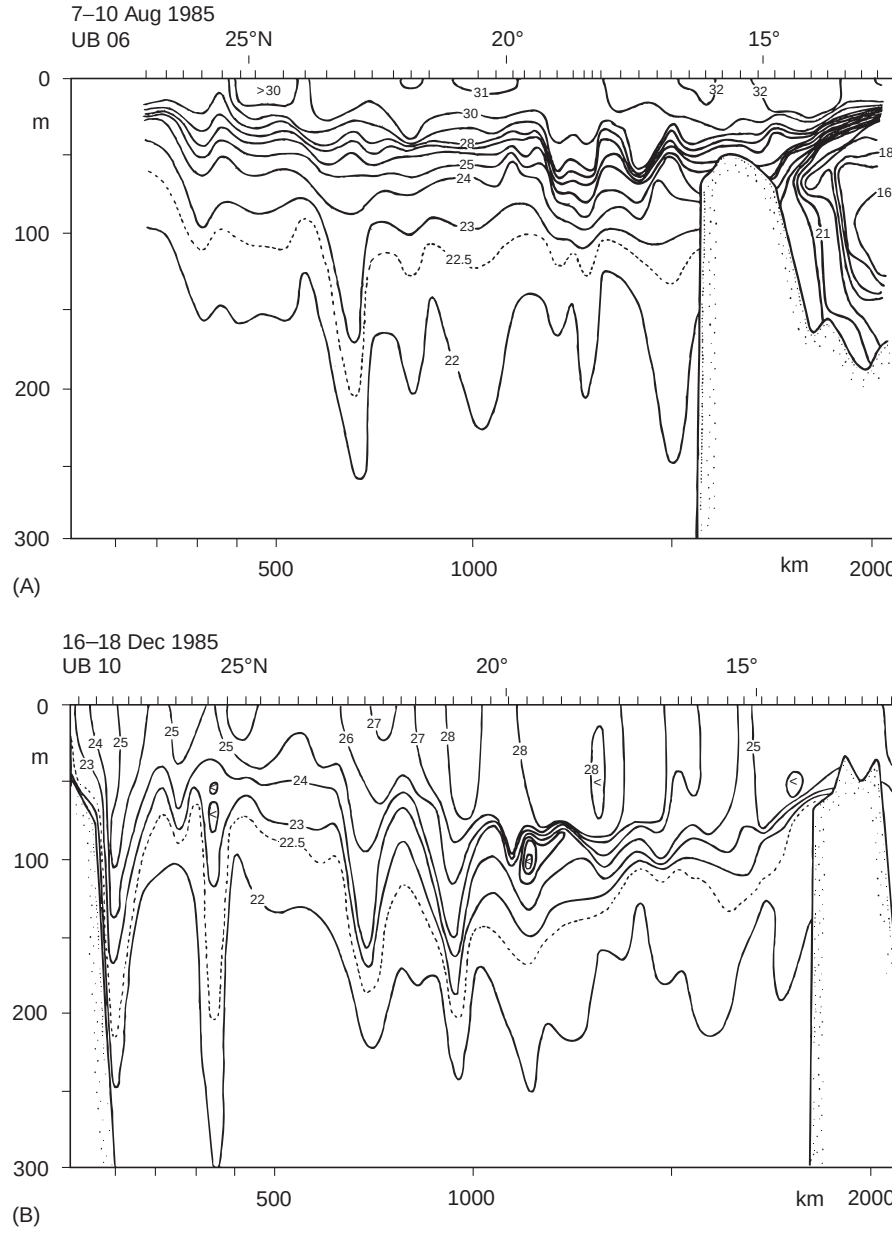

Figure 2 Distribution of temperature (°C) along the axis of the Red Sea in the upper 300 m during the two monsoon seasons in (A) August and (B) December, based on measurements with expendable bathythermographs.

major part of the outflow at the bottom of the strait of Bab El Mandeb. In contrast during the summer the temperature stratification in the southern part of the Red Sea is unstable. A cold wedge penetrates below the shallow mixed layer from the Gulf of Aden into the Red Sea and outflows of warmer water exist above and below. This cold wedge has been observed as far north as 20°N. This three-layer structure in the southern Red Sea is caused by the northerly monsoon winds, which during the summer season between June and August drive the surface water out of the Red Sea.

The full depth hydrographic section shown in **Figure 3** was taken during October 1982. In the upper layer the structure is still that of the southwest monsoon, with an intrusion of cold and low salinity water at intermediate depths. Surface temperatures are highest just north of Bab El Mandeb (~32°C) decreasing to 27°C in the north, and surface salinities increase from 37.5 PSU in the strait to more than 40 PSU in the north. Compared to these changes in the upper layer the deep water temperatures and salinities are almost homogeneous with values of 21.6°C for temperature and 40.6 PSU

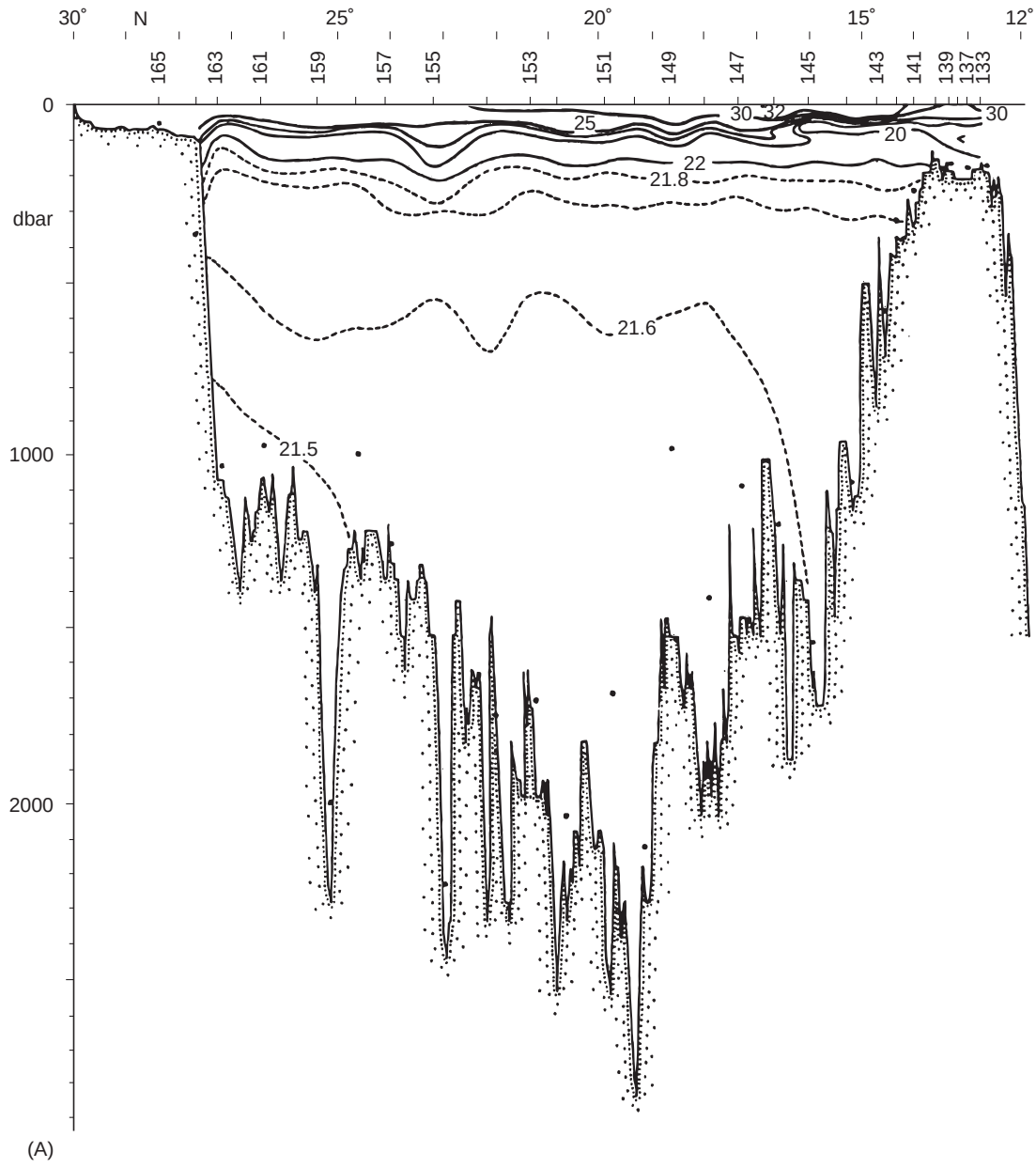

Figure 3 Vertical distribution of (A) potential temperature (°C), (B) salinity (PSU) (C), potential density and (D) dissolved oxygen content ($ml\,l^{-1}$) along the central axis of the Red Sea during October 1982.

for salinity. Horizontal differences between the northern and the southern part of the Red Sea do not exceed 0.2 K and 0.02 PSU, respectively. In contrast, the distribution of dissolved oxygen (and other chemical parameters) does show some structure in the deep water. There is a pronounced oxygen minimum around 300 m depth in the southern part of the Red Sea, whereas values are relatively high near the bottom and in the northern part. The distributions of chemical parameters have been used to evaluate the pattern and magnitude of the deep circulation. New deep water is formed in the north, it sinks to the bottom, spreads southward and upwells slowly. The intermediate depth oxygen minimum is thus a result of the balance between upwelling of Red Sea Deep Water and downward diffusion of thermocline water.

Circulation in the Upper Layer

The annual mean circulation above the pycnocline is largely driven by thermohaline forces. The excess of evaporation over precipitation results in a loss of $0.03 \times 10^6\,m^3\,s^{-1}$ and forces a near surface inflow

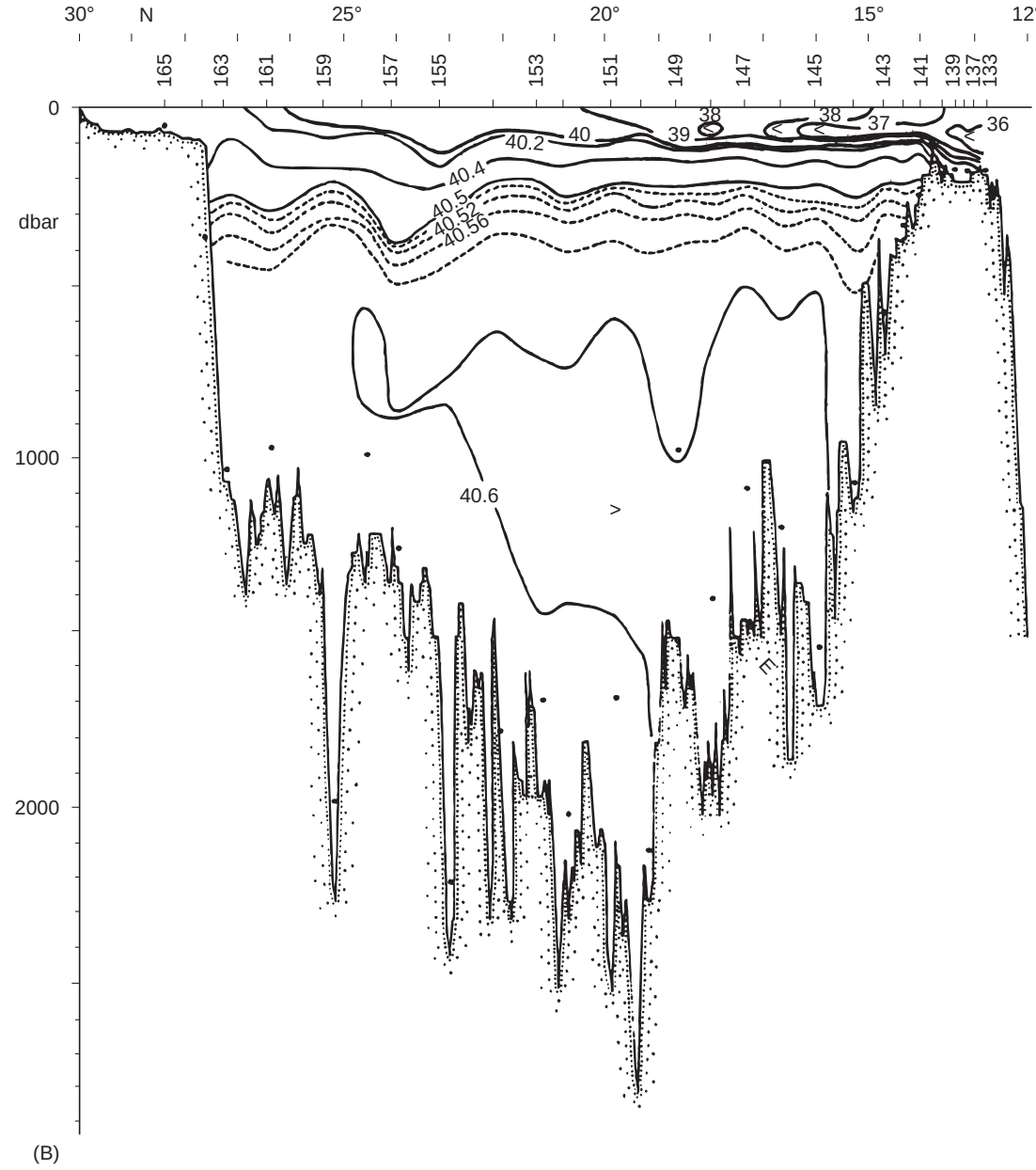

Figure 3 (continued)

through the Strait of Bab El Mandeb. Applying Knudsen's formula and balancing mass and salt fluxes through the strait and the sea surface results in an overall strength of the circulation and thus an outflow into the Gulf of Aden of $0.33 \times 10^6\,m^3\,s^{-1}$. Direct measurements of the exchanges in the strait have confirmed this number.

These mean conditions have been successfully modeled as a turbulent convective flow driven by a constant buoyancy flux B_0 at the sea surface. The surface currents scale with $(B_0^2 x)^{1/3}$ where x is the distance from the inner boundary of the estuary, and the overturning circulation is confined to the layer above sill depth. Superimposed on this pattern is the wind-driven circulation forced by the seasonally changing monsoon winds. It leads to a southward surface flow in the southern part of the Red Sea during summer. The inflow compensating the two outflows at the surface and at the bottom then occurs at intermediate depths and a three-layer system develops in and north of the strait. During winter the wind enforces the thermohaline circulation, resulting in the classical two-layer system. Linear inverse box models applied to hydrographic

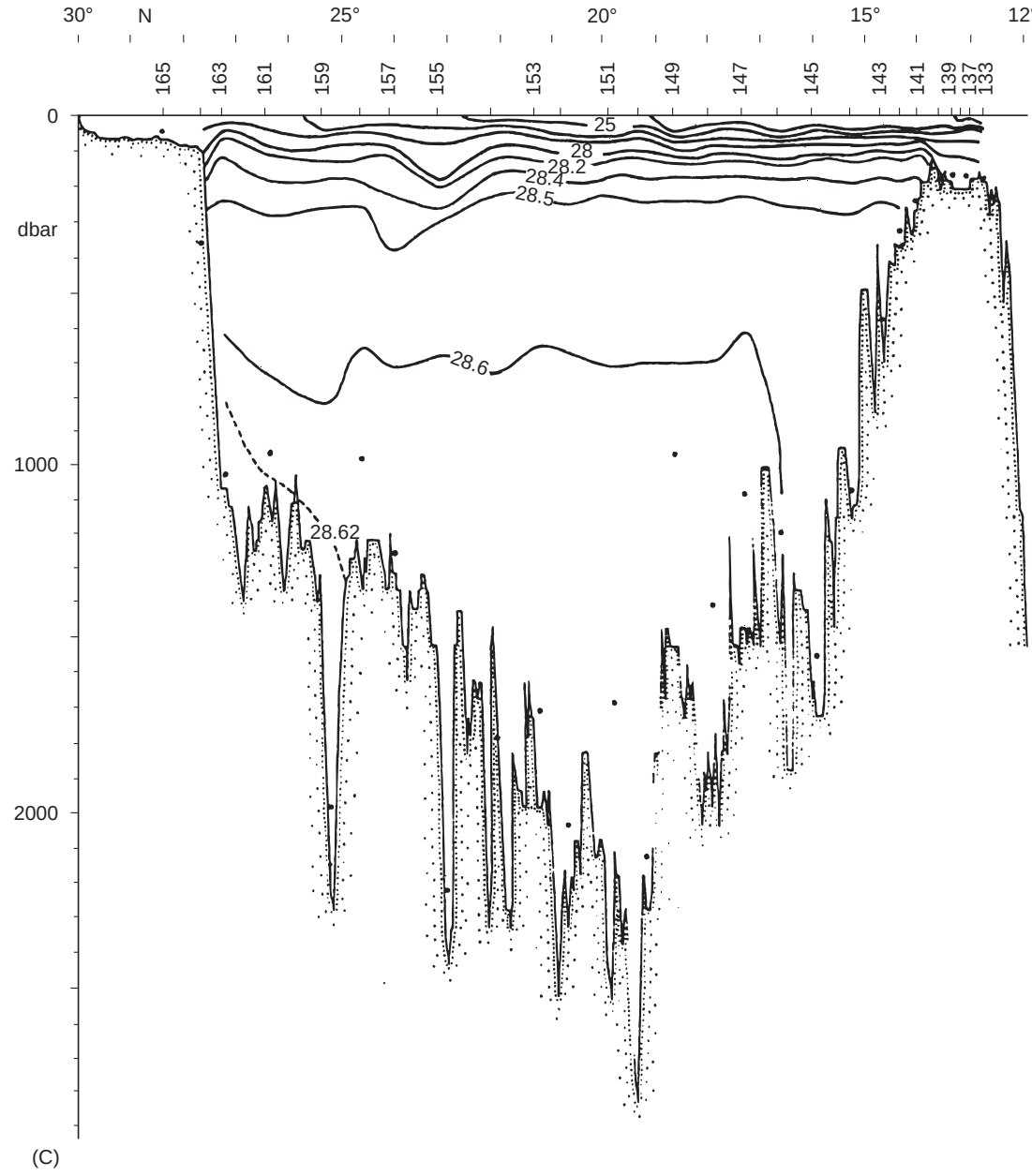

Figure 3 (continued)

and chemical data have in principle also been able to reproduce the overturning circulation and confirmed the dominant role of the buoyancy forcing over the wind forcing. However, due to the lack of geo-chemical data the details of the upper circulation have not been delineated. Only few direct current measurements have been made within the Red Sea proper, outside the strait regions, and the above described surface circulation patterns are mainly based on ship drift observations. In general, mean near surface current speeds do not exceed $0.1\,\mathrm{m\,s^{-1}}$ except in the southern narrows of the sill region and the strait of Bab El Mandeb.

This two-dimensional description of the upper layer circulation is, however, incomplete. Along-axis hydrographic sections show strong depressions of the thermo- and haloclines with horizontal scales of the basin width, which are superimposed on the mean hydrographic structure (**Figures 2** and **3**). The depressions, indicative of anticyclonic eddies or gyres, are mostly found in regions where the Red Sea widens, i.e. around 18°N, 20°N and 23°N. The gyres have also been seen in the few direct current measurements available and are associated with transports of up to $3 \times 10^6\,\mathrm{m^3\,s^{-1}}$, an order of magnitude larger than those of the mean circulation. It

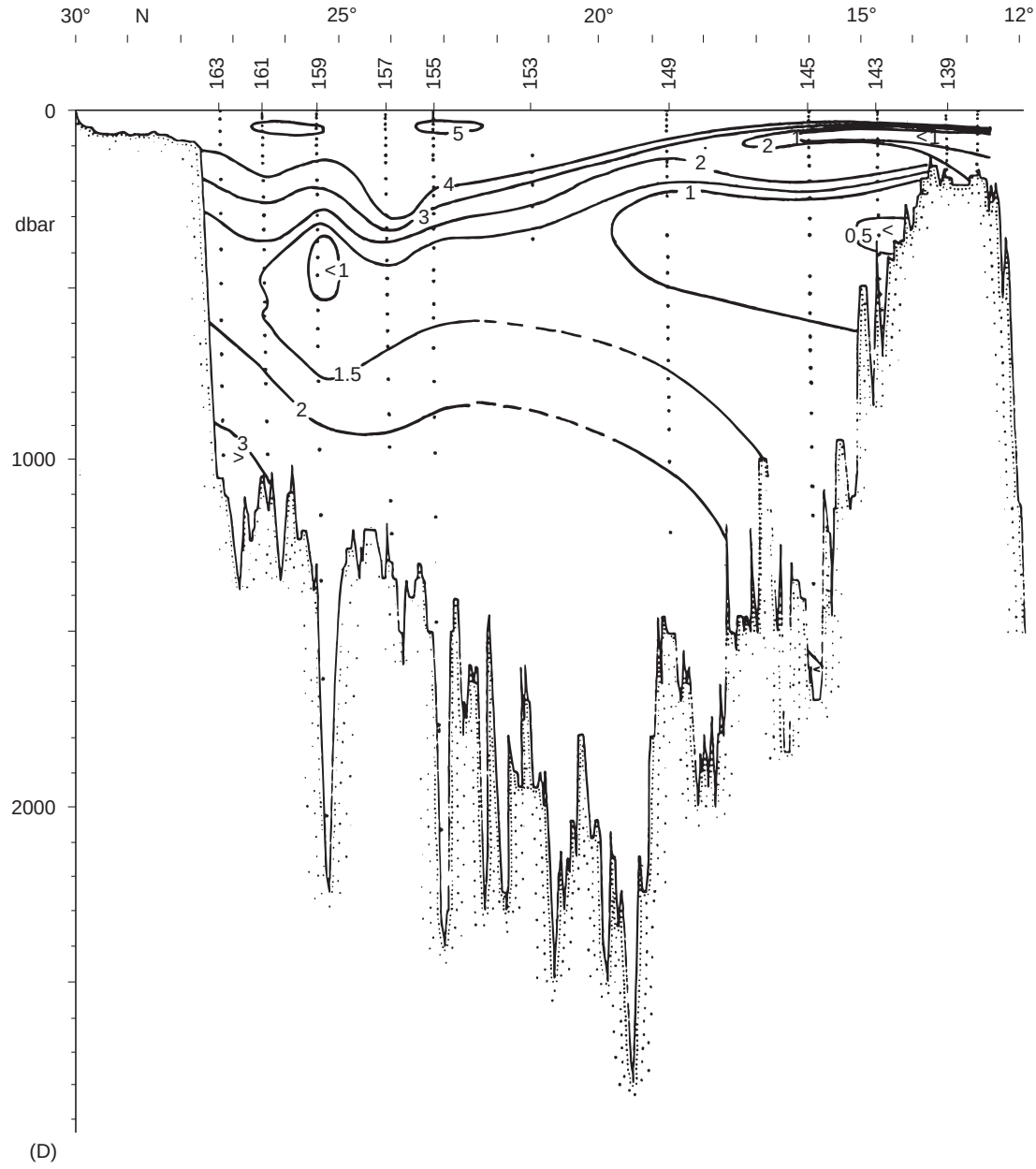

Figure 3 (continued)

has been suggested that they are formed through the strong rotational wind field over the Red Sea and are locked in by the topography. Also high-resolution three-dimensional circulation models have recently been used to simulate the current patterns in the Red Sea in more detail. Probably the most important result of these studies is the prediction of narrow boundary currents, at both the western and eastern coasts, that partly detach from the boundary to form closed circulation cells in the interior. The large-scale meridional pressure gradient caused by evaporation is suggested as a driving force for the boundary currents.

Deep Circulations

The renewal and circulation of the deep water of the Red Sea has attracted more scientific research than the surface circulation. Temperature and salinity in the deep layer of the Red Sea are almost homogeneous (**Figures 2 and 3A, B**), pointing towards a sluggish renewal, but the high degree of oxygen saturation of more than 50% near the bottom suggests just the opposite.

Three different sources for the deep water in the Red Sea were proposed based on observations made during the International Indian Ocean Expedition of

the 1960s: outflow and plume convection of winter bottom water from the Gulf of Suez; overflow and plume convection of intermediate water from the Gulf of Aqaba; and open ocean convection and subduction south of the Sinai Peninsula. The individual contributions of these sources could not be established, but the overall deep water renewal was estimated to $0.06 \times 10^6\,m^3\,s^{-1}$ by fitting hydrographic data of the interior of the Red Sea to a simple one-dimensional vertical advection–diffusion model. This transport value corresponds to a residence time of the deep water of about 70 years. Other estimates were based on the decay of radioactive tracers or on analytical modeling studies. These gave somewhat longer timescales of up to 300 years for the deep water renewal. Finally, short-term direct current measurements in the dense winter outflows from the Gulf of Suez and from the Gulf of Aqaba showed transports of 0.08 and $0.03 \times 10^6\,m^3\,s^{-1}$, respectively. Adding a mixing contribution to the descending plumes led to renewal times of the deep water of the order 100 years.

More recently the ventilation of the deep water and the associated circulation has been studied using a variety of linear two-dimensional box models, inverting hydrographic and geochemical tracer data. Although differing in detail, these models estimate renewal timescales of only 30–40 years and suggest a ventilation of the upper deep water through open ocean convection and subduction and of the lower deep water through slope convection fed by the outflows from the two gulfs.

All these estimates of the deep water renewal are either based on mean climatological data or on sets of measurements that can be considered synoptic with respect to the calculated residence times. They use information on tracer history and decay or short-term current measurements. Variability in the deep water formation is not considered.

Intermittency of the deep water renewal has been demonstrated based on a time series of hydrographic data separated by one or several winters. During a survey in May 1983, just seven months after the homogeneous structure shown in **Figure 3** was observed, the Θ–S characteristics in the northern part of the Red Sea had changed drastically whereas in the southern part only marginal differences were observed. Between the slope of the Gulf of Suez and about 25°N deep water temperatures had dropped by up to 0.3 K (**Figure 4**), the salinity distribution showed a parallel freshening of up to 0.06 PSU and the oxygen content had increased by $0.5\,ml\,l^{-1}$. Cooler and fresher water has entered this regime and mixed with the older deep water of the previous year. Since the lowest temperatures were found near the bottom, the deep-water renewal took place in the form of plume convection caused by dense outflow of bottom water from the Gulf of Suez, plunging down the northern continental slope. Four years later, during summer 1987, this newly formed water had spread southward along the entire Red Sea, having ventilated the deep basin within less than a decade. This sets a lower limit on the near bottom currents of $1–2\,cm\,s^{-1}$.

The renewal of the Red Sea Deep Water and its circulation may thus be summarized as follows (**Figure 5**). The deeper part of the basin below about 600 m is ventilated by slope convection fed by the outflows from the Gulf of Suez and the Gulf of Aqaba. Due to the large reservoir of the Gulf of Aqaba the latter outflow is more steady and provides the more permanent source for the deep water. The density of the winter water in the Gulf of Suez shows strong interannual variability and its contribution to the deep basin of the Red Sea is thus intermittent. These two sources feed a southward bottom current which upwells and in part recirculates northward above the bottom flow. The upper deep water is ventilated through shallow plume convection, when the bottom waters of the adjacent shelves are not dense enough to sink to the bottom of the Red Sea, and through open ocean convection south of the Sinai peninsula. Both sources feed a southward flow that merges with the southward flow of the lower thermocline in the interior of the basin and make up the outflow of Red Sea Water through the Strait of Bab El Mandeb.

Exchanges with the Gulf of Aden

The Strait of Bab El Mandeb is about 150 km long and connects the Red Sea with the Gulf of Aden and the Indian Ocean. With the 163 m deep sill near the Hanish Islands in the north and the 18 km wide Perim Narrows in the south it is a bottleneck for the exchange between both basins. Both locations are candidates for hydraulic control of the water exchange.

The buoyancy driven large-scale overturning circulation of the Red Sea supports a two-layer exchange through the strait, with an inflow at the surface and an outflow of dense water at the bottom. Simple budget calculations for the Red Sea point toward an inflow at a mean rate of $0.36 \times 10^6\,m^3\,s^{-1}$ and outflow of $0.33 \times 10^6\,m^3\,s^{-1}$ balancing the annual mean freshwater loss and keeping the overall salt content of the Red Sea constant.

The local wind field over the southern Red Sea modifies this picture and strengthens the exchange

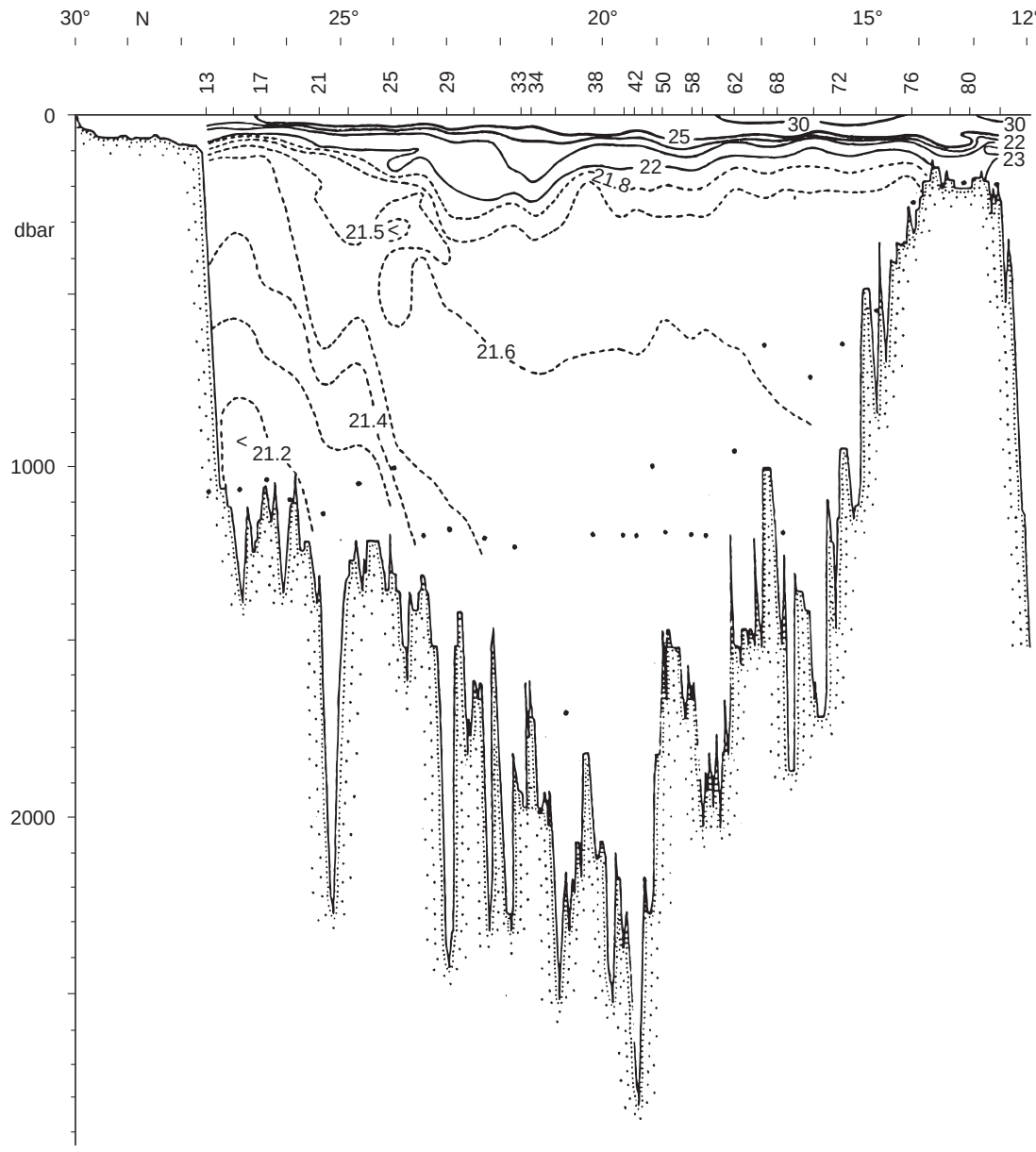

Figure 4 Vertical distribution of potential temperature (°C) along the central axis of the Red Sea during May 1983. Dots mark the maximum depth of measurements at the respective station.

during winter, when winds blow towards the north. During the height of summer, between June and August, the southward blowing winds force a shallow outflow of surface water from the Red Sea and cause upwelling in the Gulf of Aden. This sets up a northward pressure gradient which drives the cold inflow at intermediate depths, sandwiched between the surface and the bottom outflows. These layered structures of the throughflow and their seasonal modulation has been documented during a number of hydrographic surveys and from some short-term current measurements with moored instrumentation, carried out since the 1960s. More recently an almost complete seasonal cycle has been documented with a ten months mooring array.

The total exchange through the strait varies between a high of $0.7 \times 10^6\,m^3\,s^{-1}$ during February and a low of $0.35 \times 10^6\,m^3\,s^{-1}$ during August, the deep outflow of high salinity Red Sea Water changes from 0.7 to less than $0.05 \times 10^6\,m^3\,s^{-1}$ between those seasons (**Figure 6**). This means that during the three to four month long summer season the fluxes are mainly associated with the wind-driven upper circulation cell rather than with the thermohaline

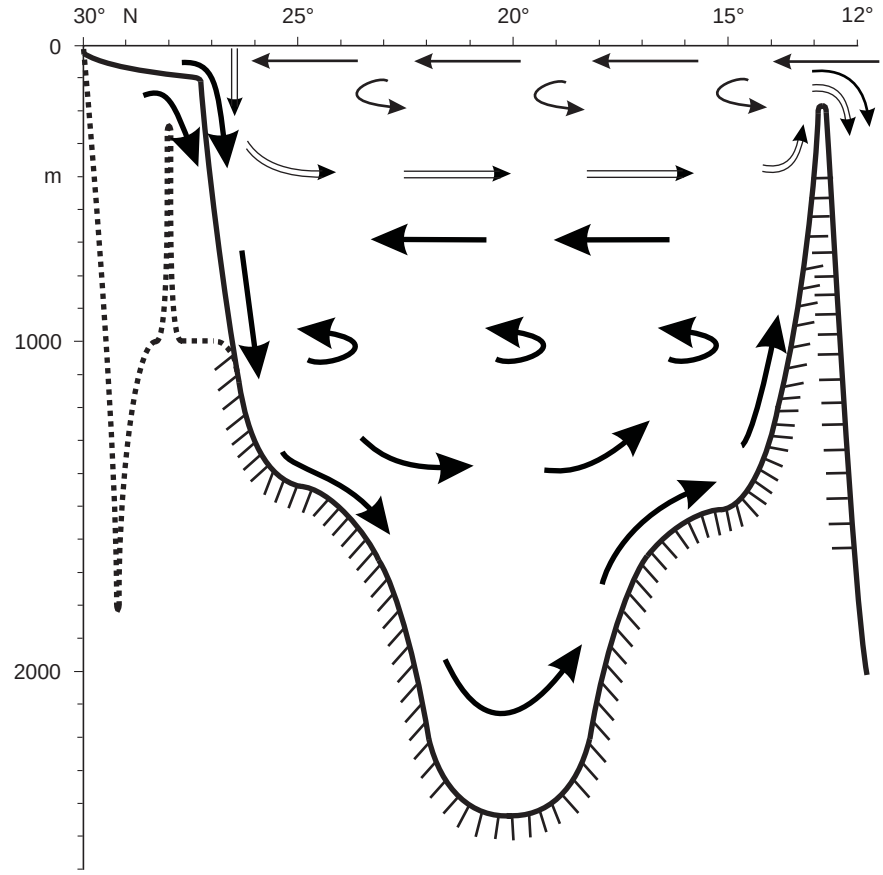

Figure 5 Schematic of the circulation in the upper and deep water layers in the Red Sea. Light arrows indicate the circulation cell in the upper layer, double arrows that of the upper deep water that is driven by open ocean convection and bold arrows the deep circulation driven by plume convection. The circulation pattern is based on interpretation of hydrographic data and few direct current observations. The dotted topography in the north is that of the Gulf of Aqaba.

overturning driving the deep outflow. However, one should bear in mind, that from the observations the fluxes in the upper layers are not as well established as those in the deep outflow, due to the widening geometry of the strait and the poorer coverage with moored instruments. The mean outflow of dense Red Sea Water ($0.37 \times 10^6\,m^3\,s^{-1}$), however, corresponds closely to the prediction based on the evaporation budget.

Mean current speeds in the deep outflow vary from less than $0.2\,m\,s^{-1}$ to more than $1.0\,m\,s^{-1}$ between the seasons. Superimposed on this annual signal are shorter-term current fluctuations, from several days to weeks, that may be associated with the passage of coastal trapped waves or are caused directly by the local wind forcing. Transport variability associated with these fluctuations, are most pronounced in the winter season and can be as high as $0.4 \times 10^6\,m^3\,s^{-1}$. The strongest variability is caused by the semidiurnal tides, which reach amplitudes of $0.5\,m\,s^{-1}$ during spring conditions.

Hydraulic control does not appear to limit the exchanges through the strait on the mean seasonal cycle. In the long-term data from moored instrumentation critical or supercritical flow conditions were only seen for the second vertical mode, where internal waves propagating into the Red Sea may get arrested. This limits the outflow of upper deep Red Sea Water but does not hamper the overall exchange. The situation may, however, be different during extreme conditions associated with the passage of coastal trapped waves and/or tides.

The seasonally changing structure and strength of the flow in the strait has an impact on the water mass characteristics of the dense outflow that actually reaches the Gulf of Aden, sinks and spreads in the Indian Ocean. In the northern part of the strait, temperatures and salinities are fairly constant throughout the year, despite the changing transport rates of the outflow. In the strait towards the southern exit, vertical mixing with the overlying water reduces the salinity during both seasons, but more

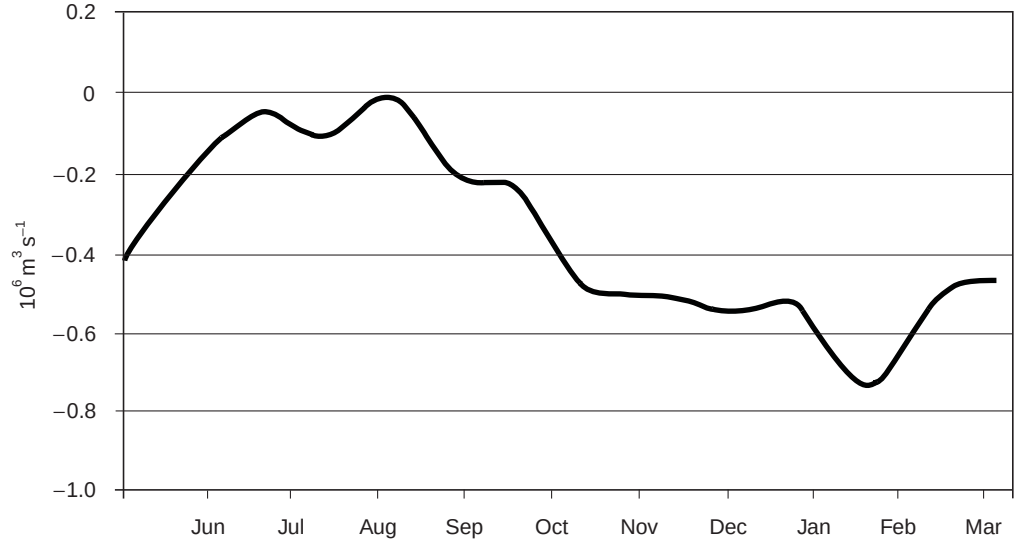

Figure 6 Time series of transport in the outflow of Red Sea Water in the Strait of Bab El Mandeb.

Table 1 Characteristics of the dense Red Sea outflow

	Summer	*Winter*
Temperature (°C)	20.7	22.9
Salinity (PSU)	39.0	39.9
Density ($kg\,m^{-3}$)	27.63	27.69
Transport ($10^6\,m^3\,s^{-1}$)	0.05	0.70

so in summer, and leads to a warming in winter and a cooling in summer (**Table 1**). The seasonal change in the density of the outflow is, however, small, as these two effects almost cancel each other. In the Gulf of Aden the dense Red Sea Water sinks down the continental slope to a depth of equilibrium density, primarily along two channels in the topography. During descent in the two channels mixing with the ambient water of the Gulf of Aden reduces the density further and dilutes the Red Sea Water by a factor of about three. The endproducts then spread at depths of around 700 m and 1100 m.

Conclusions

The basic dynamics of the circulation of the Red Sea, both for the upper stratified layer and in the nearly homogeneous deep trench, have been known since the 1960s. Heat and freshwater fluxes associated with the strong evaporation lead to the formation of the highly saline Red Sea Water and drive both the shallow overturning circulation above sill depth and the deep circulation. The latter is forced through deep convection in the far north of the Red Sea. More recently the ventilation time of the deep water was calculated by use of geochemical tracers fitted to box models. Estimates converge on around 30 years, but it has also been found that deep convection is intermittent and a strong convection event can renew the deep water within less than a decade. The exchanges between the Red Sea and the Indian Ocean, in particular its seasonal variability, have also recently been quantified. The outflow of dense Red Sea Water varies between $0.05 \times 10^6\,m^3\,s^{-1}$ in summer and $0.70 \times 10^6\,m^3\,s^{-1}$ in winter, with an annual mean of $0.37 \times 10^6\,m^3\,s^{-1}$. The exchanges are not limited by hydraulic control and thus the Gulf of Aden/Indian Ocean might influence the dynamics of the Red Sea. The possible remote forcing of the Red Sea circulation from the Indian Ocean and a better understanding of its variability remain a challenging aspect of future Red Sea research.

See also

Current Systems in the Indian Ocean. Flows in Straits and Channels. Thermohaline Circulation. Wind Driven Circulation.

Further Reading

Cember RP (1988) On the sources, formation and circulation of Red Sea deep water. *Journal of Geophysical Research* 93: 8175–8191.

Pratt LJ, Johns W, Murray SP and Katsumata K (1999) Hydraulic interpretation of direct velocity measurements in the Bab al Mandab. *Journal of Physical Oceanography* 29(11): 2769–2784.